Article

Thiolate Bridging and Metal Exchange in Adducts of a Zinc Finger Model and Pt Complexes: Biomimetic Studies of Protein/Pt/DNA Interactions

Elky Almaraz, Queite A. de Paula, Qin Liu, Joseph H. Reibenspies, Marcetta Y. Darensbourg, and Nicholas P. Farrell

J. Am. Chem. Soc., **2008**, 130 (19), 6272-6280 • DOI: 10.1021/ja711254q • Publication Date (Web): 19 April 2008

J|A|C|S
ARTICLES

Published on Web 04/19/2008

Thiolate Bridging and Metal Exchange in Adducts of a Zinc Finger Model and Pt^{II} Complexes: Biomimetic Studies of Protein/Pt/DNA Interactions

Elky Almaraz,[†] Queite A. de Paula,[‡] Qin Liu,[‡] Joseph H. Reibenspies,[†] Marcetta Y. Darensbourg,[†] and Nicholas P. Farrell*[,‡]

Department of Chemistry, Texas A&M University, College Station, Texas 77843, and Department of Chemistry, Virginia Commonwealth University, Richmond, Virginia, 23284-2006

Received January 3, 2008; E-mail: npfarrell@vcu.edu

Abstract: To provide precedents for the possible interactions of platinum DNA adducts with *zinc finger* proteins, the complexes [Pt(dien)Cl]Cl (dien = diethylenetriamine) and [Pt(terpy)Cl]Cl (terpy = 2,2′:6′,2″-terpyridine) were exposed to the *N,N*′-bis(2-mercaptoethyl)-1,4-diazacycloheptanezinc(II) dimer, $[Zn(bme\text{-}dach)]_2$, and the products defined by electrospray ionization mass spectrometry (ESI−MS), X-ray crystallography and ^{195}Pt NMR spectroscopy. The presence of a leaving chloride in both platinum(II) complexes facilitates electrophilic substitution involving sulfur-containing zinc finger synthetic models or, as in previous studies, zinc finger peptidic sequences. Monitored via ESI−MS, both reactants yielded evidence for Zn−(μ-SR)−Pt bridges followed by zinc ejection from the N_2S_2 coordination sphere and subsequent formation of a trimetallic Zn−(μ-SR)$_2$−Pt−(μ-SR)$_2$−Zn-bridged species. The isolation of Zn−(μ-SR)−Pt-bridged species [(Zn(bme-dach)Cl)(Pt(dien))]Cl is, to our knowledge, the first Zn−Pt bimetallic thiolate-bridged model demonstrating the interaction between Zn-bound thiolates and Pt^{2+}. In the case of the [Pt(terpy)Cl]Cl reaction with the $[Zn(bme\text{-}dach)]_2$, ESI−MS analysis further suggests metal exchange by formation of $[Zn(terpy)Cl]^+$, whereas the [Pt(dien)Cl]Cl reaction does not yield the corresponding $[Zn(dien)Cl]^+$ ion. Direct synthesis of the Zn−Pt thiolate-bridged species and the Pt(N_2S_2) chelate, where Pt has displaced the Zn from the chelate core, permitted the isolation of X-ray-quality crystals to confirm the bridging and metal-exchanged structures. The ESI−MS, ^{195}Pt NMR spectroscopy, and molecular structures of the di- and trinuclear complexes will be discussed, as they provide insight into the metal-exchange mechanism.

Introduction

Critical biological functions regulated by the docking of cysteine-rich zinc finger proteins onto DNA or RNA include DNA repair, regulation of genetic transcription, and viral−host-cell incorporation.[1–3] These important biomolecule interactions may be inhibited upon chemical modification, usually alkylation or oxidation, of the zinc-binding ligands. Such chemical modification may result eventually in zinc ejection and loss of protein tertiary structure, resulting in the inhibition of biological function. Especially in the case of the HIV nucleocapsid zinc-finger NCp7 protein, this strategy has been used to develop small-molecule inhibitors as a potentially new class of HIV-inhibiting drugs.[4–6] A formal analogy exists between alkylation and platination (metalation); chemical modification of the biomolecular substrate involves in both cases electrophilic attack on the cysteinyl sulfurs of the zinc-binding site. In agreement, *in vitro* studies using mass spectrometry and other spectroscopic techniques have demonstrated the ability of platinum-nucleobase compounds, such as *trans*-$[PtCl(9\text{-}EtGua)(pyr)_2]^+$ and *[SP-4-2]*-$[PtCl(9\text{-}EtGua)(NH_3)(quin)]^+$, to bind to the C-terminal domain of the NCp7 peptide with subsequent ejection of the zinc.[7,8] It is reasonable to suggest that the mechanism of zinc ejection also involves platination of zinc-binding ligands within the active site, analogous to alkylation, with the formation at some point of a ligand-bridged Zn−Pt species. In support, the reaction between *cis*-$[PtCl_2(NH_3)_2]$ (*cis*-DDP, cisplatin) and a 31 amino acid zinc finger sequence containing a $ZnCys_4$-binding site proceeds in a stepwise manner in the presence of 2 equiv of *cis*-DDP with complete deligation of Zn^{2+}.[9]

The concept of ternary Zn (protein)/Pt/(DNA/RNA) species may have widespread relevance in biology. Recognition of cisplatin-adducted DNA is seen for many proteins, a number

[†] Texas A&M University.
[‡] Virginia Commonwealth University.

(1) Venter, J. C.; Adams, M. D.; Myers, E. W.; Li, P. W.; Mural, R. J.; Sutton, G. G. *Science* **2001**, *291*, 1304–1351.
(2) Schwabe, J. W. R.; Klug, A. *Nat. Struct. Biol.* **1994**, *1*, 345–349.
(3) Berg, J. M.; Shi, Y. *Science* **1996**, *271*, 1081–1085.
(4) Musah, R. A. *Curr. Top. Med. Chem.* **2004**, *4*, 1605–1622.
(5) Huang, M.; Maynard, A.; Turpin, J. A.; Graham, L.; Janini, G. M.; Covell, D. G.; Rice, W. G. *J. Med. Chem.* **1998**, *41*, 1371–1381.
(6) Stephen, A. G.; Worthy, K. M.; Towler, E.; Mikovits, J. A.; Sei, S.; Roberts, P.; Yang, Q.; Akee, R. K.; Klausmeyer, P.; McCloud, T. G.; Henderson, L.; Rein, A.; Covell, D. G.; Currens, M.; Shoemaker, R. H.; Fisher, R. J. *Biochem. Biophys. Res. Commun.* **2002**, *296*, 1228–1237.
(7) Anzellotti, A. I.; Liu, Q.; Bloemink, M. J.; Scarsdale, J. N.; Farrell, N. *Chem. Biol.* **2006**, *13*, 1–10.
(8) Sartori, D. A.; Miller, B.; Bierbach, U.; Farrell, N. *J. Biol. Inorg. Chem.* **2000**, *5*, 575–583.
(9) Bose, R. N.; Wei, W.; Yang, W.; Evanics, F. *Inorg. Chim. Acta* **2005**, *358*, 2844–2854.

10.1021/ja711254q CCC: $40.75

of which contain the Zn-finger motif.[10–12] Two relevant human examples are the XPA repair protein and the transcription factor Sp1. DNA–protein crosslinking reactions involving zinc finger proteins and site-specific platinated oligonucleotides have also been described. Tetra- and trifunctional dinuclear platinum complexes cross-link the Sp1 protein and components of the bacterial UvrABC repair system to DNA−DNA *interstrand* adducts induced by the complexes.[13–15] Heterodinuclear [Pt,Ru] compounds are also capable of inducing these ternary DNA–protein cross-links.[14,16] Incorporation of steric hindrance into an ethylenediamine chelate allows for ternary DNA–protein cross-linking of an initially formed monofunctional DNA adduct with components of the UvrABC repair system, because of retardation of the second (bifunctional) DNA-binding step and favorable competitive reaction with protein.[17] The use of *trans*-DDP to cross-link the zinc finger nucleocapsid protein to HIV-1 RNA may proceed through a similar mechanistic pathway.[18]

As stated, the molecular description of ternary DNA–protein complexes involving zinc fingers and platinated DNA may reasonably be considered to involve a zinc-binding site (cysteine) bridging to a platinated nucleobase (polynucleotide). The well-known affinity of platinum(II) compounds for sulfur certainly suggests the feasibility of Zn−(μ-SR)−Pt intermediates in these biological processes. The mechanism of zinc ejection may also involve such intermediates. The alkylation/platination analogy has also been successful in studying model reactions where potential Zn−Pt intermediates were observed by mass spectrometry. Initial results from a study of the zinc protein model $[Zn(bme\text{-}dach)]_2$ (a structural drawing shown in Scheme 3) and *trans*-$[PtCl(9\text{-}EtGua)(pyr)_2]^+$ showed the formation of putative Zn−Pt species and eventual incorporation of Pt into the chelate to form [Pt(bme-dach)].[19] Such a small-molecule study may be predictive of chemical models for the proposed biological structures. The earlier biomolecule and mass spectral studies may be considered to be on the micro−nanomolar scale, wherein the reaction between zinc finger synthetic analogues and simple platinum and platinum−nucleotide complexes might mimic the more complicated biological system. In pursuing these analogies, we have made a tandem study at the millimolar (bulk chemical synthesis) level for the purpose of adduct and proposed intermediate isolation, which may be structurally characterized, including X-ray diffraction studies. The latter technique will give detailed information on the feasibility of the possible bonding arrangements in the biological system. A schematic of the possibilities is presented in Scheme 1. This paper reports on the study of two representative platinum compounds $[Pt(dien)Cl]^+$ and $[Pt(terpy)Cl]^+$ with $[Zn(bme\text{-}dach)]_2$.

Scheme 1. Possible Products Resulting from the Interactions of Zinc-Bound Thiolates with Pt^{2+} Species

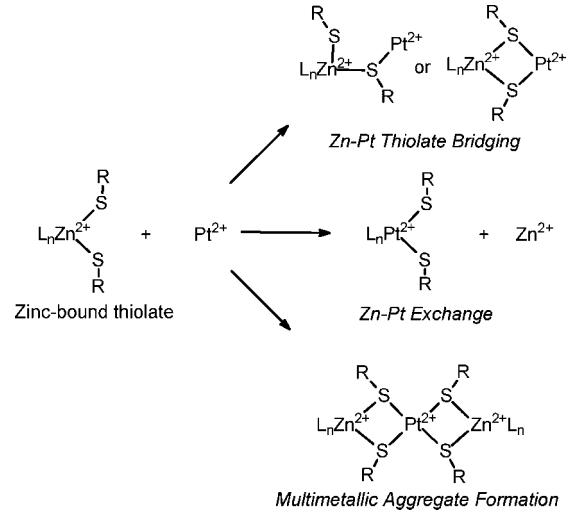

2. Experimental Section

2.1. Materials and Reagents. The complexes [Pt(terpy)Cl]Cl and [Pt(dien)Cl]Cl were prepared from K_2PtCl_4 as described before.[20] The purity of the complexes was confirmed by ^1H and ^{195}Pt NMR spectroscopy and elemental analyses, which were performed by QTI Laboratory, Whitehouse, NJ, the Canadian Microanalytical Services, Ltd., Delta, British Columbia, Canada, or Atlantic Microlab, Inc., Norcross, GA. All reagents and reactants were used without further purification.

2.2. Synthesis of *N*,*N*′-Bis(2-mercaptoethyl)-1,4-diazacycloheptanezinc(II) Dimer, [Zn(bme-dach)]$_2$, Complex I. The bis(2-mercaptoethyl)-1,4-diazacycloheptane (H_2bme-dach) ligand was prepared according to published procedures.[21] Under N_2, H_2bme-dach (2.530 g, 11.5 mmol) was dissolved in 20 mL of MeOH and sodium methoxide (1.220 g, 22.6 mmol) in 20 mL of MeOH was slowly added. The solution was vigorously stirred for 2 h at 22 °C. Under N_2, $ZnCl_2$ (1.568 g, 11.5 mmol) dissolved in 35 mL of MeOH was rapidly added to the stirring solution and immediately formed a white precipitate. After 28 h of stirring under an N_2 blanket, the white solid was isolated by filtration in air and washed 3 times with MeOH to yield, after drying *in vacuo*, 2.64 g (4.7 mmol) of $[Zn(bme\text{-}dach)]_2$ product (81.7% yield). The dimer was dissolved in pyridine and layered with diethyl ether to yield colorless X-ray quality crystals. ESI−mass spectrum: $[M + H]^+$ $m/z = 569$. Elemental analysis: calculated (found) C, 38.1 (37.8); H, 6.39 (6.13); N, 9.87 (9.83).

2.3. Synthesis of *N*,*N*′-Bis(2-mercaptoethyl)-1,4-diazacycloheptanezincchloride Platinum Diethylentriamine [(Zn(bme-dach)Cl)(Pt(dien))]Cl, Complex III. Under N_2, the $[Zn(bme\text{-}dach)]_2$ (0.0258 g, 0.0455 mmol) was dissolved in 30 mL of MeOH and heated to 37 °C with stirring. The [Pt(dien)Cl]Cl (0.0330 g, 0.0894 mmol) was dissolved in 3 mL of deionized H_2O and added dropwise to the clear, colorless $[Zn(bme\text{-}dach)]_2$ solution. The cloudy reaction mixture was stirred at 37−39 °C for 39 h, after which time the stirring was stopped to allow the grayish precipitate to settle. The precipitate was removed by filtration, and the clear colorless solution was concentrated *in vacuo*. X-ray quality crystals were obtained through both layering and vapor diffusion with MeOH/diethyl ether. Approximate yield from recrystallization tubes: 0.016 g (0.024 mmol), 27%. ESI−mass spectrum: $[M]^+$ $m/z = 616$, $[M - Cl]^{2+}$ $m/z = 290.5$. ^{195}Pt NMR spectroscopy: –3267.95 ppm.

(10) Kartalou, M.; Essigmann, J. M. *Mut. Res.* **2001**, *478*, 1–21.
(11) Wang, D.; Lippard, S. J. *Nat. Rev. Drug Discovery* **2005**, *4*, 307–320.
(12) Sancar, A. *Annu. Rev. Biochem.* **1999**, *65*, 43–81.
(13) Farrell, N.; Qu, Y.; Roberts, J. D. Multifunctional DNA-binding metal complexes. In *Topics in Biological Inorganic Chemistry*; Clarke, M. J., Sadler, P. J., Eds.; Springer: New York, 1999; pp 99–115.
(14) Van Houten, B.; Illenye, S.; Qu, Y.; Farrell, N. *Biochemistry* **1993**, *44* (32), 11794–11801.
(15) Kloster, M.; Kostrhunova, H.; Zaludova, R.; Malina, J.; Kasparkova, J.; Brabec, V.; Farrell, N. *Biochemistry* **2004**, *43*, 7776–7786.
(16) Qu, Y.; Farrell, N. *Inorg. Chem.* **1995**, *13* (34), 3573–3576.
(17) Lambert, B.; Jestin, J. L.; Brehin, P.; Oleyowski, C.; Yeung, A.; Mailliet, P.; Pretot, C.; le Pecq, J. B.; Jacquemin-Sablon, A.; Chottard, J. C. *J. Biol. Chem.* **1995**, *36* (270), 21251–21257.
(18) Darlix, J. L.; Gabus, C.; Nugeyre, M. T.; Clavel, F.; Barre-Sinoussi, F. *J. Mol. Biol.* **1990**, *216*, 689–699.
(19) Liu, Q.; Golden, M.; Darensbourg, M. Y.; Farrell, N. *Chem. Comm.* **2005**, *34*, 4360–4362.
(20) Annibale, G.; Brandolisio, M.; Pitteri, B. *Polyhedron* **1995**, *3* (14), 451–462.
(21) Smee, J. J.; Miller, M. L.; Grapperhaus, C. A.; Reibenspies, J. H.; Darensbourg, M. Y. *Inorg. Chem.* **2001**, *40*, 3601–3605.

Elemental analysis: calculated (found) C, 23.91 (22.83); H, 4.79 (5.18); N, 10.73 (10.58). Note: Shorter reaction times were used in attempts to isolate the monothiolate-bridged species, **II**. However, crystals of the dithiolate-bridged species were the sole product.

2.4. Synthesis of *N*,*N*′-Bis(2-mercaptoethyl)-1,4-diazacycloheptaneplatinum(II), [Pt(bme-dach)], Complex IV. Under a N_2 atmosphere, H_2bme-dach (0.306 g, 1.39 mmol) was dissolved in 15 mL of MeOH and KOH (0.158 g, 2.82 mmol) in 10 mL of MeOH was added to it slowly. The solution was stirred vigorously for 1.5 h. A portion of K_2PtCl_4 (0.579 g, 1.39 mmol) was dissolved in a 30 mL of solvent mixture comprised of 10 mL of MeOH and 20 mL of H_2O and slowly added to the stirring solution. The reaction mixture was stirred vigorously at room temperature overnight, after which time the bright yellow solution and solid were separated. The solid was washed with 20 mL of MeOH, and all washings were added to the solution. The solution was then reduced in volume *in vacuo* and placed on a silica gel chromatography column, with MeOH as the eluant. The first pale yellow band was collected and dried to yield 0.040 g of pure product, a 7.0% yield. X-ray quality crystals were obtained from slow evaporation from a concentrated MeOH solution. ESI−mass spectrum: $[M + H]^+$ $m/z = 414$, $[M + Na]^+$ $m/z = 436$, $[M + K]^+$ $m/z = 452$. ^{195}Pt NMR spectroscopy: –3044.4 ppm. Elemental analysis: calculated (found) C, 26.14 (25.17); H, 4.39 (4.27); N, 6.78 (6.56).

2.5. Synthesis of *N*,*N*′-Bis(2-mercaptoethyl)-1,4-diazacycloheptane-zincchloroplatinate, [Zn(bme-dach)Cl]$_2$Pt, Complex V. Two methods were implemented to produce (a) pure product in the form of insoluble powder and (b) X-ray-quality crystals for molecular structure determination.

(a) A solution of K_2PtCl_4 (0.0215 g, 0.052 mmol) in 5 mL of H_2O was added to $[Zn(bme\text{-}dach)]_2$ (0.0297 g, 0.052 mmol) dissolved in 35 mL of MeOH. After stirring for ca. 2 h, the yellow precipitate was isolated by filtration and washed with H_2O, MeOH, and Et_2O to remove any starting materials or salts. The yellow solid was dried *in vacuo*; yield, 0.0210 g (48.7%). The product was found to be partially soluble in tetrahydrofuran (THF) and $CHCl_3$. ESI−mass spectrum: $[M - Cl]^+ = 797$ m/z. ^{195}Pt NMR spectroscopy: –3472.50 ppm. Elemental analysis: calculated (found) C, 25.94 (25.57); H, 4.35 (4.36); N, 6.72 (6.25).

(b) Stock solutions of K_2PtCl_4 (0.0630 g, 0.152 mmol) in 6 mL of H_2O/MeOH (80/20 V) and $[Zn(bme\text{-}dach)]_2$ (0.0155 g, 0.027 mmol) in 30 mL of MeOH/MeCN (67/33 V) were prepared. A total of 1 mL (0.025 mmol) of the K_2PtCl_4 solution was transferred to a Schlenk tube and layered carefully with 2 mL of MeOH. The $[Zn(bme\text{-}dach)]_2$ solution (25 mL or 0.023 mmol) was then delicately layered above the MeOH layer. The tube was then held at 2 °C for 3 days, after which time the pale yellow needles that developed at the interface were harvested for X-ray diffraction study.

Isolation from NMR Experiments. When the reaction between [Pt(dien)Cl]Cl and $[Zn(bme\text{-}dach)]_2$ in either a 1:1 or a *2Pt:1Zn* molar ratio was monitored by ^{195}Pt NMR spectroscopy, yellowish crystals precipitated within the NMR tube after ca. 2 h. Upon filtration and drying, elemental analysis showed the formation of the species corresponding to $[Zn(bme\text{-}dach)Cl]_2Pt$; calculated (found) C, 25.94 (25.89); H, 4.35 (4.36); N, 6.72 (6.52).

2.6. Sample Preparations for ESI−MS Analysis. A 100 μL sample of 0.01 mM methanolic solution of $[Zn(bme\text{-}dach)]_2$ was mixed with 100 or 200 μL of 0.01 mM water solutions of [Pt(dien)Cl]Cl or [Pt(terpy)Cl]Cl, respectively, and incubated at 37 °C. ESI−MS spectra were recorded by taking a 10 μL solution mixture and diluting with 100 μL of MeOH, prior to injection into the mass spectrometer. Mass spectrometry (ESI−MS) on the directly synthesized $[Zn(bme\text{-}dach)]_2$ and complexes **III**, **IV**, and **V** were performed by the Laboratory for Biological Mass Spectrometry at Texas A&M University.

2.7. Electrospray Ionization Mass Spectrometry (ESI−MS). Electrospray ionization mass spectra were recorded with a Finnigan LCQ ion-trap electrospray meter (LCQ−MS) in positive-ion mode. The voltage at the electrospray needles was 4.5 kV, and a N_2 sheath gas and Aux/sweep gas were used. The capillary was heated to 150 °C. The solutions were injected into the ESI source directly at a flow rate of 3.0 μL/min. Tandem mass and zoom scan were used to analyze the structure of the product in the experiments. Helium was admitted directly into the ion-trapping efficiency and as the collision gas in the collision-induced dissociation (CID) experiment. A maximum ion injection time of 500 ms along with 10 scans was set. To induce collision activation, the relative collision energy was controlled to 10–30% of the maximum, depending upon the precursor ions and MS*n*. In MS/MS and MS*n* experiments, an isolation width of 6–12 *m*/*z* units for the precursor ions was used to allow the signature Pt isotopic distribution to be observed.

2.8. NMR Spectroscopy. ^{1}H and ^{195}Pt NMR spectra were obtained on a Varian 300 MHz NMR spectrometer (Virginia Commonwealth University) at 23 °C, using 5 mm NMR tubes. The chemical shifts (δ) in the ^{1}H NMR spectra were referenced from 98% D_2O (4.79 ppm). The ^{195}Pt chemical shifts were referenced to K_2PtCl_4 in D_2O (−1614 ppm).

2.9. X-ray Structure Analysis. Low-temperature (110 K) X-ray diffraction data were collected on a Bruker SMART 1000 CCD based diffractometer (Texas A&M University) (Mo Kα radiation, $\lambda = 0.710\,73$ Å) for the Pt(bme-dach) single crystal.[22] The [(Zn(bme-dach)Cl)(Pt(dien))]Cl data were collected on the Bruker-AXS APEX-II CCD 3-thircle X-ray diffractometer under the same conditions. For the $[Zn(bme\text{-}dach)]_2$ and $[Zn(bme\text{-}dach)Cl]_2Pt$ complexes, data were obtained on a Bruker D8 GADDS general-purpose three-circle X-ray diffractometer (Cu Kα radiation, $\alpha\lambda = 1.541\,84$ Å), also operating at 110 K. The structures were solved by direct methods. H atoms were added at idealized positions and refined with fixed isotropic displacement parameters equal to 1.2 times the isotropic displacement parameters of the atoms to which they were attached. Anisotropic displacement parameters were determined for all non-hydrogen atoms. Programs used were as follows: data collection and cell refinement, *SHELXTL*;[23] absorption correction, *SADABS*; structure solution, *SHELXS-97* (Sheldrick);[24] structure refinement, *SHELXL-97* (Sheldrick);[25] and molecular graphics and preparation of material for publication, *SHELXTL-PLUS*, version 5.1 or later (Bruker). X-seed was employed for the final data presentation and structure plots.[26] Table S1 in the Supporting Information lists the crystallographic data for the four compounds included in this paper.

3. Results

The reaction between $[Pt(dien)Cl]^+$ and the Zn dithiolate complex $[Zn(bme\text{-}dach)]_2$ was studied using ESI−mass spectrometry, ^{195}Pt NMR spectroscopy, and X-ray crystallography on isolated products. Scheme 2 lists the compounds that were characterized in this study. The molecular structures of complexes **I**, **III**, **IV**, and **V** were determined by X-ray diffraction analysis and that of complex **II** was inferred by ^{195}Pt NMR spectroscopy.

ESI−MS Analysis of the Reaction between [Pt(dien)Cl]Cl and [Zn(bme-dach)]$_2$, Reaction 1. When probed by ESI−mass spectrometry, the reaction between [Pt(dien)Cl]Cl and $[Zn(bme\text{-}dach)]_2$ gave rise to two new major peaks, which remained invariant with time (Figure 1a). The *m*/*z* values of 290.9 and

(22) SMART 1000 CCD; Bruker Analytical X-ray Systems: Madison, WI, 1999.
(23) Sheldrick, G. SHELXTL-PLUS, reVision 4.11V, SHELXTL-PLUS Users Manual; Siemens Analytical X-ray Instruments, Inc.: Madison, WI, 1990.
(24) Sheldrick, G. SHELXS-97, Program for Crystal Structure Solution; Universitaẗ Gottingen: Gottingen, Germany, 1997.
(25) Sheldrick, G. SHELXL-97, Program for Crystal Structure Refinement; Universitaẗ Gottingen: Gottingen, Germany, 1997.
(26) Barbour, L. J. *J. Supramol. Chem.* **2001**, *1*, 189–191.

Scheme 2. Compounds **II**, **III**, **IV**, and **V** Formed in the Reaction between $[Pt(dien)Cl]^+$ and the Zn Model $[Zn(bme\text{-}dach)]_2$, Complex **I**

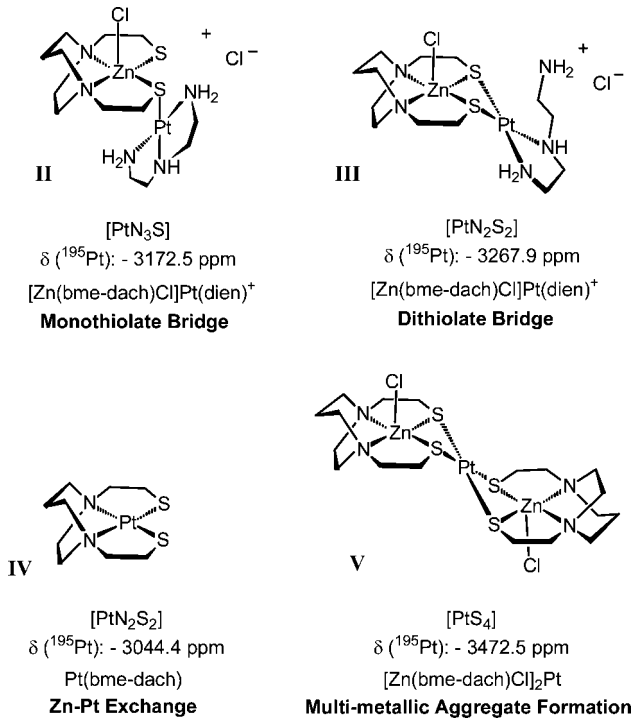

Scheme 3. Reaction Pathways of the $[Zn(bme\text{-}dach)]_2$ with [Pt(dien)Cl]Cl and [Pt(terpy)Cl]Cl and the Formation of Thiolate-Bridged, Metal-Exchanged, and Multimetallic Aggregate Species

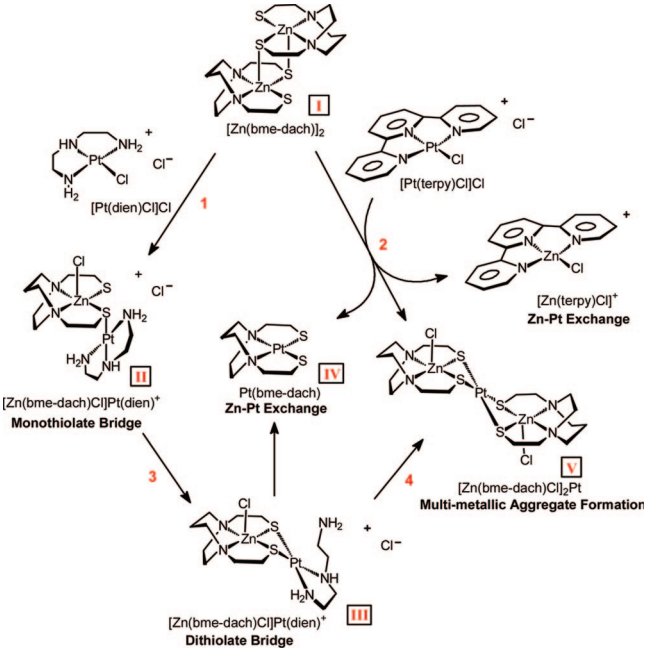

616.3 were assigned to the species corresponding to $[Zn(bme\text{-}dach)(Pt(dien))]^{2+}$ and $[(Zn(bme\text{-}dach)Cl)(Pt(dien))]^{+}$, respectively. The isotopic distributions of these two peaks agree with the calculated predictions (see Figure S1 and S2 in the Supporting Information). The minor peaks shown in Figure 1a at m/z = 432.80 and 574.70 may be ascribed to formulations such as $[(Zn(bme\text{-}dach))_2Pt(dien)]^{2+}$ and $[(Zn(bme\text{-}dach))_3Pt(dien)]^{2+}$, respectively. The formation of higher molecular-weight Zn−Pt clusters of the type $[(Zn(bme\text{-}dach))_nPt]^{2+}$, with n = 2–8, has been observed via ESI−MS when the complexes *cis*-$[Pt(NH_3)_2(guanosine)_2]^{2+}$ or *trans*-$[Pt(py)_2(9\text{-}EtGH)_2]$ were incubated with $[Zn(bme\text{-}dach)]_2$.[7]

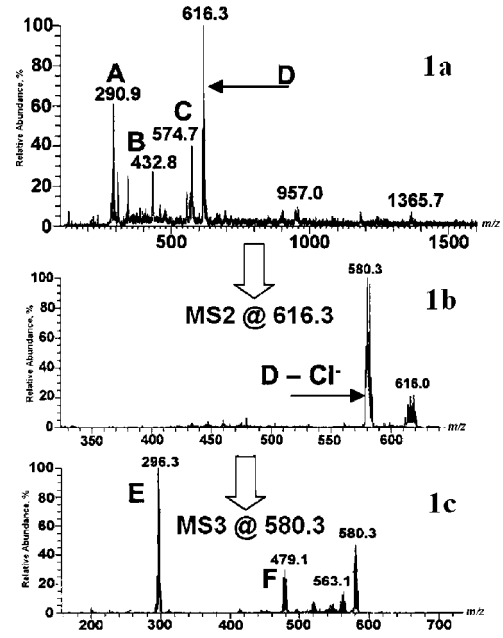

Figure 1. ESI−MS spectrum of a 1:1 mixture of [Pt(dien)Cl]Cl and $[Zn(bme\text{-}dach)]_2$ (1a) after 48 h of incubation, showing the predominant species $[Zn(bme\text{-}dach)Pt(dien)]^{2+}$ (A), $\{[Zn(bme\text{-}dach)]_2Pt(dien)\}^{2+}$ (B), $\{[Zn(bme\text{-}dach)]_3Pt(dien)\}^{2+}$ (C), and $\{[Zn(bme\text{-}dach)Cl]Pt(dien)\}^{+}$ (D). The MS2 spectrum of D exhibits the D−Cl^- species (1b), and the MS3 at 580.3 yields $[Pt(dien)–H^+]^+$ (E) and $[Zn(bme\text{-}dach)Pt–H^+]^+$ (F) (1c).

The composition of the major species was further explored with CID experiments to assess the sites of bridging and cleavage. The MS2 of the peak at 616.2 (Figure 1b) resulted in the daughter ion at 580.3, consistent with the loss of chloride from $[(Zn(bme\text{-}dach)Cl)(Pt(dien))]^{+}$. As shown in Figure 1c, the MS3 fragmentation of the signal at 580.3 then produces two parent ions with m/z 296.3 and 479.1, which may be assigned to the ions $[Pt(dien)]^{+}$ and $[Zn(bme\text{-}dach)Pt]^{+}$, respectively. The dominant peak at 616.3 thus corresponds to the very stable heterodinuclear species $[(Zn(bme\text{-}dach)Cl)(Pt(dien))]^{+}$, indicative of the high affinity of platinum(II) compounds to sulfur.[7]

^{195}Pt NMR Spectroscopic Analysis of Reaction 1: Evidence of a Monothiolate-Bridged Intermediate and Dithiolate-Bridged Product. ESI−mass spectrometry cannot distinguish between the putative structures **II** and **III**. The reactions and nature of the products were further explored by NMR spectroscopy. The ^{195}Pt NMR spectrum of the [Pt(dien)Cl]Cl gave a single peak with a chemical shift at –2280.8 ppm, as is typical of Pt^{2+} in a N_3Cl donor environment.[27] Upon reaction of 2 equiv of [Pt(dien)Cl]Cl with 1 equiv of $[Zn(bme\text{-}dach)]_2$ (i.e., 1Pt:1Zn) over the course of 30 m at 37 °C, a new ^{195}Pt NMR resonance appeared at –3172.53 ppm (Figure 2). This chemical shift is typical of a PtN_3S coordination sphere. Furthermore, after 1 h, an additional peak was observed at –3267.95 ppm, which grew in intensity with time. The downfield shift of this singlet in the ^{195}Pt NMR spectrum is consistent with a $[PtN_2S_2]$ species. After 3 h (Figure 2), this latter signal

(27) Oehlsen, M. E; Qu, Y.; Farrell, N. *Inorg. Chem.* **2003**, *18* (42), 5498–5506.

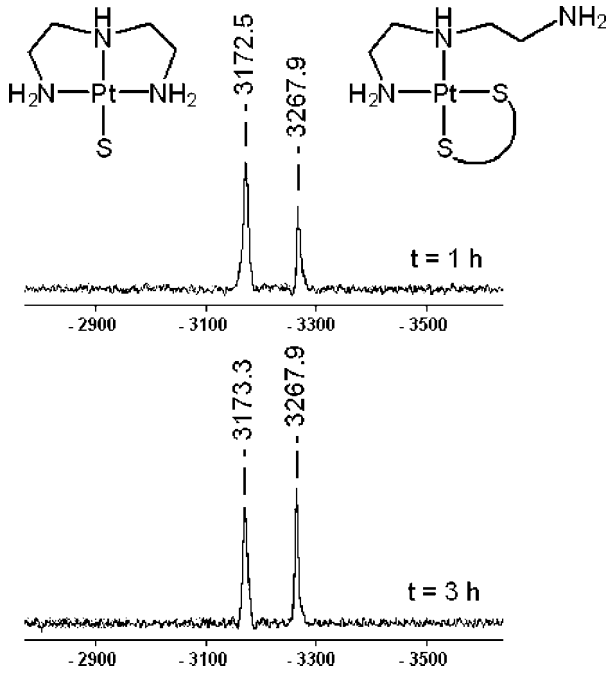

Figure 2. ^{195}Pt NMR spectra obtained from the reaction between [Pt(dien)Cl]Cl and [Zn(bme-dach)]$_2$ (2:1 ratio) after 1 h (top) and 3 h (bottom), in MeOH.

at –3267.95 ppm was clearly visible as the major component. After 2 days, the same species as observed in the 3 h spectrum were observed in the solution in a similar ratio, indicating that the reaction had attained equilibrium. The most reasonable assignments for these species are shown in Scheme 2, and in the case of complex **III**, this assignment was confirmed by X-ray crystallography.

After approximately 2 h, a yellowish precipitate appeared, which gave (after isolation and drying) an elemental analysis corresponding to [Zn(bme-dach)Cl]$_2$Pt, complex **V** (Scheme 2). The ^{195}Pt NMR spectrum of this species has a δ(Pt) chemical shift of − 3472.5 ppm and is likely to be a Pt^{2+} in a S_4 coordination sphere;[28] again, this was confirmed by X-ray crystallography.

Structural Analyses. [Zn(bme-dach)]$_2$, Complex 1, and Pt(bme-dach), Complex IV. Four compounds essential to this study were subjected to X-ray diffraction studies; crystallographic data are listed in Table 1. Ball and stick drawings of the molecular structures are shown in Figures 3, 4, 6, and 7. Figure 3 shows the [Zn(bme-dach)]$_2$ dimeric complex used as a zinc finger model in this and previous work to have a pentacoordinate zinc in N_2S_3 coordination. The dimeric partners are related such that one-half of the dimer is the symmetry-generated product of the other. In terms of pseudo-trigonal bipyramidal geometry, the N_2S_2 donor set about Zn(1) produces axial N(2) and S(1) donors with ∠N(2)−Zn−S(1) of 157°, while the equatorial trigonal plane is defined by ∠N(1)−Zn−S(2) = 128.5°, ∠N(1)−Zn−S(1)′ = 113.2°, and ∠S(2)−Zn−S(1)′ = 115.3°. The S(1)′ sulfur donor is bridging between the two partners of the dimer and would thus be in an equatorial site of a pseudo-trigonal bipyramid with respect to Zn(1). The alternate description of a distorted square pyramidal structure is also applicable according to the *tau* value of 0.47, where a value of 0 indicates a perfect square pyramid and a value of 1.00 denotes a trigonal bipyramidal geometry.[29] In this case, the S(1) and S(1)′ are in the apical positions, while the N(1), N(2), S(1), and S(2) are in a very distorted basal plane. Pertinent distance parameters are given in the caption of Figure 3.

Table 1. Selected Bond Lengths (Å) and Bond Angles (deg) for [Zn(bme-dach)Cl(Pt(dien))]Cl and [Zn(bme-dach)Cl]$_2$Pt

	[(Zn(bme-dach)Cl)(Pt(dien))]Cl	[Zn(bme-dach)Cl]$_2$Pt
Zn(1)–S(1)	2.4567(10)	2.4390(16)
Zn(1)–S(2)	2.4210(10)	2.4159(17)
Zn(1)–N(1)	2.148(3)	2.178(5)
Zn(1)–N(2)	2.167(3)	2.196(5)
Zn(1)–Cl(1)	2.2575(9)	2.2520(17)
Pt(1)–S(1)	2.3078(9)	2.3401(14)
Pt(1)–S(2)	2.3107(9)	2.3407(15)
Zn displacement from N_2S_2 plane	0.8628	0.8755, 0.8668
∠N(1)–Zn(1)–N(2)	75.1	74.9
∠S(1)–Zn(1)–S(2)	82.3	82.6
∠S(1)–Pt(1)–S(2)	88.0	86.4
∠Cl(1)–Zn(1)–S(1)	115.9	114.5
∠Cl(1)–Zn(1)–S(2)	114.4	116.6
hinge ∠[a]	107.2	104.5, 99.0

[a] Defined in the text.

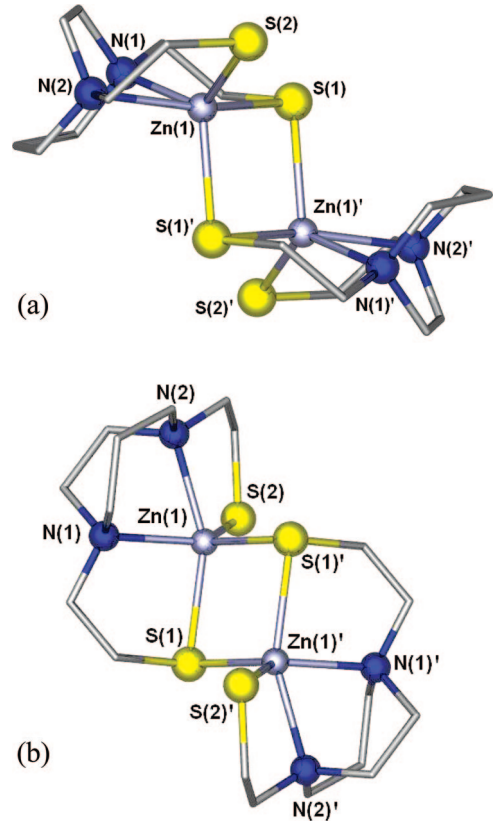

Figure 3. Ball and stick representation of the molecular structure of [Zn(bme-dach)]$_2$ emphasizing (a) square pyramidal geometry and (b) trigonal bipyramidal geometry about Zn. Selected bond lengths (Å): Zn(1)−N(1), 2.181(6); Zn(1)−N(2), 2.274(5); Zn(1)−S(1), 2.4960(17); Zn(1)−S(2), 2.3077(17); Zn(1)−S(1)′, 2.4170(16); S(1)−Zn(1)′, 2.4170(16). Selected bond angles (deg): N(1)−Zn(1)−N(2), 71.94(19); N(1)−Zn(1)−S(2), 128.51(17); N(2)−Zn(1)−S(2), 85.11(13), N(1)−Zn(1)−S(1)′, 113.18(18), N(2)−Zn(1)−S(1)′, 98.13(13), S(2)−Zn(1)−S(1)′, 115.34(7); N(1)−Zn(1)−S(1), 84.83(15); N(2)−Zn(1)−S(1), 156.62(13); S(2)−Zn(1)−S(1), 108.28(6); S(1)′−Zn(1)−S(1), 93.30(6); Zn(1)′−S(1)−Zn(1), 86.70(6).

(28) Pregosin, P. S. *Coord. Chem. Rev.* **1982**, *44*, 247–291.

(29) Addison, A. W.; Rao, T. N.; Reedijk, J.; van Rijn, J.; Verschoor, G. C. *J. Chem. Soc., Dalton Trans.* **1984**, *7*, 1349–1356.

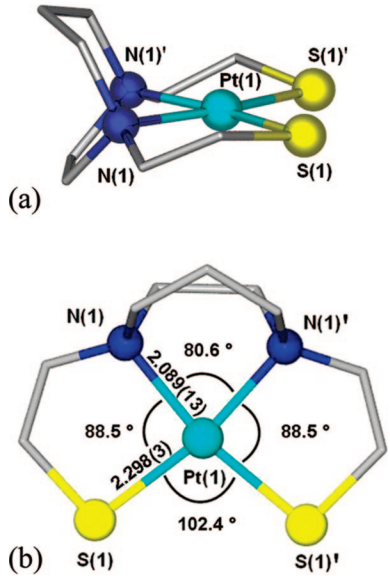

Figure 4. (a) Ball and stick representation of the Pt(bme-dach) structure and (b) alternate view displaying angles and distances.

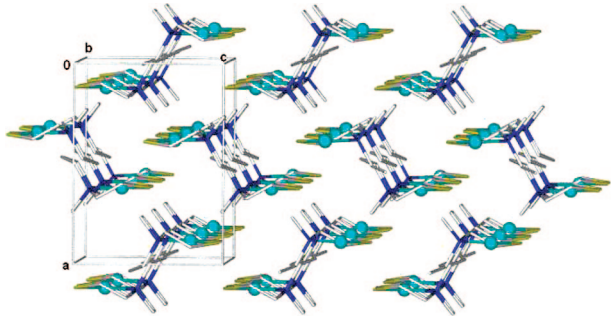

Figure 5. Packing diagram of Pt(bme-dach).

The Pt(bme-dach) molecular structure shown in Figure 4 is a highly regular square plane (deviation of Pt^{2+}) from the perfect N_2S_2 plane = 0.0003 Å. The difficulty in isolating the yellow crystals of this monomeric PtN_2S_2 compound from the insoluble yellow powder is ascribed to the presence of extended π-stacking interactions as has been seen in linear chain platinum(II) diimine complexes among others.[30–32] Nevertheless, the packing diagram (Figure 5) for monomeric Pt(bme-dach) shows no such interactions; the closest intermolecular Pt···Pt distance is 5.049 Å, while the closest $Pt\cdots S_{intermolecular}$ distance is 5.714 Å.

The effect of the large Pt^{2+} ion in the N_2S_2 donor set as contrasted to the analogous Ni(bme-dach) structure is to open the S−M−S angle by ca. 7°; i.e., for M = Ni^{2+} and Pt^{2+}, the values are 95.4° and 102.4°, respectively. A concomitant restriction of the N−Pt−N angle to 80.6° relative to the N−Ni−N angle of 82.5° is then observed.

[(Zn(bme-dach)Cl)(Pt(dien))]Cl, Complex III. Figure 6 displays the molecular structure of the dithiolate bridged [(Zn(bme-dach)Cl)(Pt(dien))]Cl, complex **III**. The extended structure of this salt (Figure S3 in the Supporting Information) finds the chloride counterion, along with H_2O and MeOH solvent

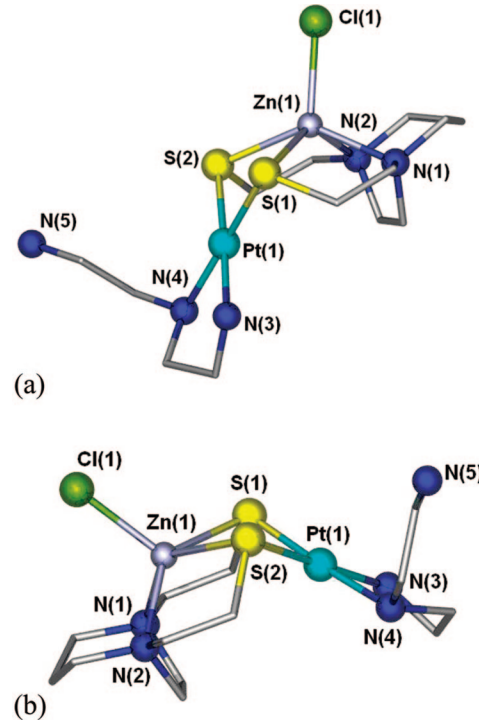

Figure 6. (a) Ball and stick presentation of the molecular structure of [(Zn(bme-dach)Cl)(Pt(dien))]Cl and (b) alternate view emphasizing the hinge angle of the dithiolate bridge.

molecules, within the unit cell. As seen in Figure 6, the Zn^{2+} is penta-coordinate, with the bme-dach N_2S_2 ligand forming the base of a square pyramid from which zinc is displaced by 0.863 Å toward a chloride that occupies the apical position of the square pyramid. Other bond distances and angles are given in Table 1. This unit serves as a metallodithiolate bidentate ligand to platinum(II), which is further coordinated by two of the three nitrogens in the diethylenetriamine ligand of the precursor $Pt(dien)Cl^+$. The alternate view of Figure 6b emphasizes the square planarity of the PtN_2S_2 unit (mean deviation within N_2S_2 plane of 0.0116 Å and Pt displacement from that plane of 0.0313 Å). The hinge at the bridging thiolate sulfurs is based on the intersection of the two best planes formed from the N(1)N(2)S(1)S(2) plane (without Zn) and the S(1)S(2)N(3)N(4) plane (without Pt) and calculated to be 107.2°.

The unit cell and the packing diagram of complex **III** are given in Figures S3 and S4 in the Supporting Information. The dangling amine experiences long-range hydrogen bonding between the amine nitrogen and the hydrogen of methanol. Further hydrogen bonding between a hydrogen of the dangling amine and the Zn-bound chloride generates a dimer of dimers. In turn, the dimer of dimers uses the other hydrogen of the dangling amine to engage the free chloride, thus forming a three-dimensional structure.

$[Zn(bme\text{-}dach)Cl]_2Pt$, Complex V. A trimetallic neutral species in which two $[ClZn(bme\text{-}dach)]^-$ units serve as bidentate metallodithiolato ligands to Pt^{2+} is the formulation of complex **V** shown in Figure 7. This structure is analogous to the slant chair or stair-step complexes seen in such complexes as $[Ni(N_2S_2)]_2M^{2+}$ (M = Ni, Pd, Pt).[33,34] It differs in that the center of the dithiolate ligand is a $ZnCl^+$ unit with the Zn^{2+} in a square

(30) Connick, W. B.; Marsh, R. E.; Schaefer, W. P.; Gray, H. B. *Inorg. Chem.* **1997**, *36*, 913–922.
(31) *Extended Linear Chain Compounds*; Miller, J. S., Ed.; Plenum Press: New York, 1982; Vol. 1−*3*.
(32) Tzeng, B. C.; Lee, G. H.; Peng, S. M. *Inorg. Chem. Commun.* **2003**, *6*, 1341–1343.
(33) Rampersad, M. V.; Jeffery, S. P.; Reibenspies, J. H.; Ortiz, C. G.; Darensbourg, D. J.; Darensbourg, M. Y. *Angew. Chem.* **2005**, *8* (44), 1217–1220.

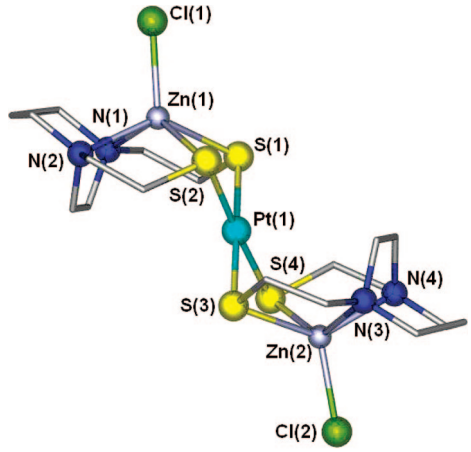

Figure 7. Ball and stick presentation of the molecular structure of [Zn(bme-dach)Cl]$_2$Pt.

pyramidal geometry, as described above. The metric parameters within the zinc coordination sphere are largely the same as those of complex **III**. These are compared in Table 1. Similar to the previous Zn−Pt dithiolate-bridged species, the hinge angle formed between the best N(1)N(2)S(1)S(2) plane (without Zn) and the S(1)S(2)S(3)S(4) plane (without Pt) is calculated to be 104.5° and that of the N(3)N(4)S(3)S(4) and S(1)S(2)S(3)S(4) planes is calculated to be 99.0°.

3.3. ESI−MS Analysis of the Reaction between [Pt(terpy)Cl]Cl and [Zn(bme-dach)]$_2$, Reaction 2: Evidence of Metal Exchange. To examine ligand effects on reactivity, the study was extended to [Pt(terpy)Cl]Cl, a square-planar complex in which the electronic and steric requirements of the rigid tridentate ligand contrasts with those of the diethylenetriamine chelate. The reactions were similarly designed at both 1:1 and 1:2 nM stoichiometry and monitored by ESI−MS. Metal-containing species were indicated by matches of appropriate isotopic distributions. The reaction is significantly more complicated than for [Pt(dien)Cl]$^+$. Table 2 shows the main species observed when dissociation and recombination processes occur for these incubated reactions. Examination of the first spectrum recorded after 5 min (Figure S5 in the Supporting Information), following mixing of the reagents in a 1:1 Zn/Pt ratio, revealed a series of Zn−Pt species as well as a ligand-scrambling reaction. Even at this early time point, signals corresponding to the reactants and also one corresponding to {[Zn(terpy)Cl] − H$^+$}$^+$ (m/z = 335.2) are clearly observed (Figure 8). The m/z envelope centered at 454.97 may be reasonably assigned to {[Pt(bme-dach)] + K$^+$} as observed for the isolated complex (see the Experimental Section). The 1:2 stoichiometry showed similar features. The principal multimetallic aggregate is {[Zn(bme-dach)]$_2$PtCl]$^+$ − H$^+$} (m/z = 797.1), and its analogue corresponding to the loss of Cl$^-$. At a Zn/Pt ratio of 1:2, the species corresponding to {[Zn(bme-dach)Pt(terpy)]$^+$ − H$^+$}$^+$ (m/z = 747.9) is observed. Spectra taken after 6 days again showed these major features to be maintained (Figure S5 in the Supporting Information). In addition, a series of minor signals detected at lower abundance and corresponding to Zn and Pt multimetallic species was observed. These include {[Zn$_3$(bme-dach)$_2$(terpy)Cl$_3$] − H$^+$}$^+$ (m/z = 974.9), {[Zn(bme-dach)]$_3$PtCl]$^+$ − H$^+$}$^+$ (m/z = 1080.9), and {[Zn(bme-dach)]$_4$PtCl]$^+$ − H$^+$}$^+$ (m/z = 1364.5) (data not shown). In accordance with Jeffery et al.,[35] the formation of these adducts containing Zn and Pt is analogous to similar polymetallic complexes using transition-metal N$_2$S$_2$ complexes, including [Zn(bme-dach)]$_2$, as metallodithiolate ligands.[33,34,36–38] Assignment of some of these peaks was assisted by MS−MS experiments, see the Supporting Information.

Table 2. Assignment of the m/z Signals in Figure8

m/z	corresponding species	calculated[a]
296.3–301.3	[Zn(terpy)]$^+$	298.7
332.3–338.3	[Zn(terpy)Cl]$^+$	335.2
462.2–468.2	[Pt(terpy)Cl]$^+$	464.8
565.0–572.0	[Zn(bme-dach)]$_2^+$	568.1
695.1–703.1	[Zn(bme-dach)$_2$Pt]$^+$	699.5
743.9–751.9	[Zn(bme-dach)Pt(terpy)]$^+$	748.4
792.8–805.8	{[Zn(bme-dach)]$_2$PtCl}$^+$	799.7
1208.08–1220.8	{[Zn(bme-dach)]$_2$[Pt$_2$(bme-dach)]Cl}$^+$	1213.5
1240.9–1255.9	{[Zn(bme-dach)]$_2$[Pt$_2$(bme-dach)]Cl$_2$}$^+$	1249.9

[a] The value given is the major signal in the isotopic bundle.

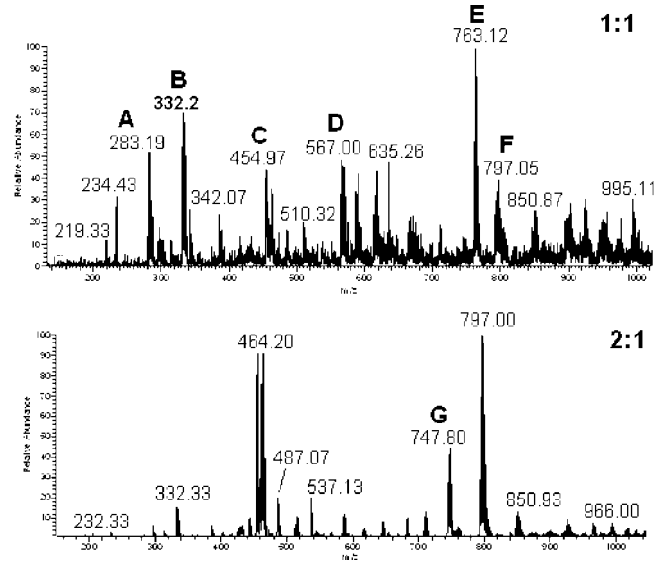

Figure 8. ESI−MS spectra full scan (positive mode) of MeOH solution containing [Pt(terpy)Cl]Cl and [Zn(bme-dach)]$_2$ in a 1:1 and 2:1 molar ratio, after 2 h of incubation at 37 °C.

4. Discussion

Small-molecule models for biologically relevant ternary DNA−Pt−zinc finger protein adducts have been characterized using ^{195}Pt NMR spectroscopy and X-ray crystallography. The isolation of Zn/Pt bimetallics, **II** and **III**, is a major advance in this area, because, to our knowledge, there are no analogous structures. In fact, the Cambridge Crystallographic Data Centre (CCDC) finds only six crystallographic structures of Zn/Pt heterometallic compounds, and those are of multimetallics with S^{2-} bridges rather than RS$^-$.[39–43] A general mechanism (see Scheme 3) for the conversion of a [PtN$_3$S] into a [PtN$_2$S$_2$]

(34) Golden, M. L.; Whaley, C. M.; Rampersad, M. V.; Reibenspies, J. H.; Hancock, R. D.; Darensbourg, M. Y. *Inorg. Chem.* **2005**, *4* (44), 875–883.

(35) Jeffery, S. P.; Green, K. N.; Rampersad, M. V.; Reibenspies, J. H.; Darensbourg, M. Y. *Dalton Trans.* **2006**, *35*, 4244–4252.

(36) Green, K. N.; Jeffery, S. P.; Reibenspies, J. H.; Darensbourg, M. Y. *J. Am. Chem. Soc.* **2006**, *19* (128), 6493–6498.

(37) Chiang, C.; Lee, J.; Dalrymple, C.; Sarahan, M. C.; Reibenspies, J. H.; Darensbourg, M. Y. *Inorg. Chem.* **2005**, *24* (44), 9007–9016.

(38) Jeffery, S. P.; Lee, J.; Darensbourg, M. Y. *Chem. Commun.* **2005**, *9*, 1122–1124.

coordination sphere has been described, as well as subsequent incorporation of Pt into the Zn model coordination sphere. Zinc preservation of cysteine thiolate nucleophilicity renders the sulfur sufficiently reactive toward electrophilic platinum moieties to yield Zn−(μ-SR)−Pt-bridged, multimetallic, and metal-exchanged species. In this respect, the chemistry is analogous to the formation of homodinuclear glutathionate (GS^-)- or cysteinate (Cys^-)-bridged Pt−RS−Pt species upon initial coordination of the thiol to a platinum center.[44–46] The tendency of coordinated Pt−GS species to form monothiolate-bridged dinuclear Pt−(μ-GS)−Pt species has been shown for $[Pt(dien)Cl]^+$, where the presence of only one leaving group in the monofunctional compound facilitated kinetic studies.[44] Crystallographic evidence for dithiolate bridging *N*-acetylcysteine is seen for the compound $[Pt_2(\mu\text{-accys-S})_2(bpy)_2]$.[45] Likewise, a bridged species has been identified as the major product from the reaction of $[PtCl_2(en)]$ with GSH.[46]

Specifically for $[Pt(dien)Cl]^+$, opening of the chelate ring is a reflection of the strong *trans* influence of cysteinate, even when modified by an interacting Zn^{2+} ion. Likewise, the formation of the trimetallic aggregate **V** is explained as a consequence of further labilization of the chelate ring under the influence of the dithiolate bridge in **III**. Note that the Pt−N bond that is broken in the tridentate dien is not that of the "central" secondary amine, i.e., the one *trans* to Cys^-. While this would lead in principle to an initial formation of a large eight-membered ring, generally considered to be unfavored, such an "opening" of the dien moiety has been previously reported through a complicated procedure involving reduction of Pt^{4+} to Pt^{2+}.[47] Should this happen here, a rapid rearrangement to give the favored five-membered ethylenediamine ring must occur. Alternatively, complex **II** may more easily result from direct displacement of the bound terminal amine by the terminal Zn−thiolate sulfur.

In the case of terpyridine, the observed formation of $[Zn(terpy)Cl]^+$ and [Pt(bme-dach)] moieties demonstrates ligand scrambling or metal ion exchange. In contrast, no $[Zn(dien)Cl]^+$ species with concomitant zinc ejection is observed in the diethylenetriamine reaction, reflecting the different steric and electronic requirements around the Zn^{2+} ion. Interestingly, Zn^{2+} and Cu^{2+} (as their chloride salts) have been shown to cleave the Pt−S bond of thiolated Pt−terpyridine to form [Pt(terpy)Cl]. A postulated mechanism involves the formation of a heterodinuclear thiolato-bridged species.[48] While these results represent a reaction in the "opposite" direction to that discussed here, nevertheless, the general system Pt(terpy)/thiolate/Cu^{2+}/Zn^{2+} appears quite reactive, supporting the possibility that the reactions reported from the mass spectrometric study can occur in solution. Further, the mass spectrometry results on the $[Pt(dien)Cl]^+$ system also correlated well with the solution behavior. One goal of this project, indeed, was to provide support for the structural interpretation of the MS data.

The heterodinuclear thiolate-bridged structures described here may represent reasonable descriptions of intermediates in metal exchange on bioligands. The exact nature of the reaction is dependent upon the choice of the ligands in the coordination sphere of platinum. Some or all of these modes of binding may be involved in zinc ejection from zinc fingers by nucleobase compounds, such as *trans*-$[PtCl(9\text{-EtGua})(pyr)_2]^+$ and *[SP-4-2]*-$[PtCl(9\text{-EtGua})(NH_3)(quin)]^+$, or indeed cisplatin itself.[7,19] These features may be general. For example, the antiarthritic gold compound, aurothiomalate, interacts with Cys_2His_2 zinc fingers of TFIIIA and Sp1 with subsequent inhibition of the DNA-binding activity of the protein.[49] Studies using a model peptide based on the third zinc finger of Sp1 confirmed that Au-binding triggered zinc release.[5] Indeed, the course of the reaction will depend upon not only the nature of the coordination sphere around platinum but also that around zinc. The chemical composition of a zinc finger core as well as the local protein environment determine the reactivity of the zinc finger.[50] The groups of Lippard, Parkin, Carrano, etc. have developed structural models of tetrahedral active sites of zinc enzymes that have also proven to be functional in their alkylation reactivity.[51] Lippard used $[Zn(SC_6H_5)_4]^{2-}$ as a mimic of the *Escherichia coli* Ada protein, responsible for repair of DNA methylphosphotriesters by methyl transfer through a zinc-activated cysteine nucleophile from a $Zn(Cys)_4$ site.[52–54] Kinetic studies of this ZnS_4 model and ZnS_xN_{4-x} species showed that the rate of methylation followed the trend: $[Zn(PhS)_4]^{2-} > [Zn(PhS)_3(MeIm)]^- \gg [Zn(PhS)_2(MeIm)_2]$. Studies by Darensbourg *et al.* have demonstrated zinc−sulfur methylation of tethered thiolates in the closely related $[Zn(bme\text{-}daco)]_2$ complex and its Cd analogue.[55] Grapperhaus *et al*. also investigated the reactivity of a similar monomeric $Zn(N_2S_2)$ complex toward alkylation and oxygenation, in which zinc-bound thiolates were alkylated by MeI and underwent oxygenation and release of Zn^{2+} in the presence of H_2O_2.[56,57] These studies point to the capability of zinc-bound thiolates to serve as active nucleophiles toward carbon electrophiles. The platination with the $[Pt(dien)Cl]^+$ and $[Pt(terpy)Cl]^+$ moieties described above further strengthens the analogy between alkylation and platination of the Zn−thiolate bond. Whether such chemistry could occur with a platinated purine or pyrimidine moiety is under investigation.

The structures described in this paper also represent viable chemical descriptions for potential ternary Pt−DNA–protein complexes involving zinc fingers and platinated DNA. The labilization of the chelate diethylenetriamine by the Zn−RS^-

(39) Li, Z.; Loh, Z. H.; Fong, S. W. A.; Yan, Y. K.; Henderson, W.; Mok, K. F.; Hor, T. S. A. *J. Chem. Soc., Dalton Trans.* **2000**, *7*, 1027–1031.
(40) Li, Z.; Zheng, W.; Liu, H.; Mok, K. F.; Hor, T. S. A. *Inorg. Chem.* **2003**, *42*, 8481–8488.
(41) Bridson, J. H.; Henderson, W.; Nicholson, B. K.; Hor, T. S. A. *Inorg. Chim. Acta* **2006**, *359*, 680–684.
(42) Capdevila, M.; Carrasco, Y.; Clegg, W.; Coxall, R. A.; Gonzalez-Duarte, P.; Lledos, A.; Ramirez, J. A. *J. Chem. Soc., Dalton Trans.* **1999**, *17*, 3103–3113.
(43) Novio, F.; Mas-Balleste, R.; Gallardo, I.; Gonzalez-Duarte, P.; Lledos, A.; Vila, N. *Dalton Trans.* **2005**, *16*, 2742–2753.
(44) Djuran, I. M.; Lempers, E. L. M.; Reedijk, J. *Inorg. Chem.* **1991**, *30*, 2648–2652.
(45) Mitchell, K. A.; Streveler, K. C.; Jensen, C. M. *Inorg. Chem.* **1993**, *32*, 2608–2609.
(46) del Sucorro Murdoch, P.; Kratochwil, N. A.; Parkinson, J. A.; Patriarca, M.; Sadler, P. J. *Agnew. Chem., Int. Ed.* **1999**, *38*, 2949–2951.
(47) Mochida, I.; Mattern, J. A.; Bailar, J. C., Jr *J. Am. Chem. Soc.* **1975**, *11* (97), 3021–3026.
(48) Cheng, C.-C.; Lu, Y.-L. *Chem. Commun.* **1998**, 253–254.
(49) Larabee, J. L.; Hocker, J. R.; Hanas, J. S. *Chem. Res. Toxicol.* **2005**, (18), 1943–1954.
(50) Maynard, A. T.; Covell, D. G. *J. Am. Chem. Soc.* **2001**, *123*, 1047–1058.
(51) Parkin, G. *Chem. Rev.* **2004**, *104*, 699–767.
(52) Wilker, J. J.; Lippard, S. J. *Inorg. Chem.* **1997**, *36*, 969–978.
(53) Myers, L. C.; Terranova, M. P.; Ferentz, A. E.; Wagner, G.; Verdine, G. L. *Science* **1993**, *261*, 1164–1167.
(54) Myers, L. C.; Wagner, G.; Verdine, G. L. *J. Am. Chem. Soc.* **1995**, *117*, 10749–10750.
(55) Grapperhaus, C. A.; Tuntulani, T.; Reibenspies, J. H.; Darensbourg, M. Y. *Inorg. Chem.* **1998**, *37*, 4052–4058.
(56) Grapperhaus, C. A.; Mullins, C. S.; Kozlowski, P. M.; Mashuta, M. S. *Inorg. Chem.* **2004**, *43*, 2859–2866.
(57) Grapperhaus, C. A.; Mullins, C. S.; Mashuta, M. S. *Inorg. Chim. Acta* **2005**, *358*, 623–632.

group further suggests a possible mode of chemical DNA repair. Glutathione has also been shown to chemically remove monofunctional Pt−DNA adducts.[58,59] The molecular description of these events implies a labilization of GS−Pt−L axis, where L is a DNA base, usually guanine. The chemistry described here suggests that $Zn-Cys^-$ could easily replicate the features of the glutathione. Additional studies pursue this interesting possibility.

A further relevant feature is the observation of several examples of five-coordinate zinc. The predictive power of bioinorganic chemistry lies to some extent in the use of model chemistry to suggest possible unexpected biological motifs. In this work, the formation of five-coordinate zinc complexes is a prevailing feature of N_2S_2Zn upon the reaction with platinum electrophiles. While it is true that the nature of the tetradentate N_2S_2 ligand produces some constraints against the tetrahedral geometry, as also evidenced by the axial ligation in the Zn dimer precursor itself, it is provocative to think that zinc fingers may use a four- or five-coordinate "coordination switch" in exercising some of their biological functions. In previous studies, species corresponding to five-coordinate Zn-9-EtGua adducts were observed when the reactions of the C-terminal NCp7 zinc finger peptide from HIV nucleocapsid protein with *trans*-$[PtCl(9\text{-}EtGua)(pyr)_2]^+$ and 9-EtGua itself were followed by ESI−MS.[7] In further agreement, a species corresponding to an adduct analogous to complex **II** has been observed in the reaction of [Pt(dien)Cl]Cl and the same C-terminal zinc finger NCp7 (Farrell, unpublished observations). The lack of a specific coordination number and geometry about zinc evidenced by this work undoubtedly relates to the metal-exchange properties of such biomimetic systems. This is consistent with Vahrenkamp's stated perspective on nature's use of zinc: "the non-properties of zinc are the basis of its success".[60] While these "non-properties" are well-known to coordination chemists, in biological chemistry, the usual view of zinc in zinc finger proteins is of a four-coordinate, tetrahedral complex. In this study, the binding of chloride, that generates a penta-coordinate anionic complex arguably increases the nucleophilicity of the thiolate sulfurs.[52] It is of interest to see if some of the biology exercised by zinc can be attributed to this facet of its coordination chemistry. These and other questions raised here present a rich area of yet to be explored bioinorganic chemistry.

Acknowledgment. The authors gratefully acknowledge the financial support of The National Institutes of Health (N.P.F.) and The National Science Foundation CHE-0616768 to N.P.F. and CHE-0616695 to M.Y.D. M.Y.D. acknowledges contributions from the R. A. Welch Foundation (A-0924). The authors acknowledge Missy Golden for the initial synthesis and structural characterization of $[Zn(bme\text{-}dach)]_2$. We also thank Atilio I. Anzellotti and John B. Mangrum for the ESI−MS discussions. Cambridge Crystallographic Data Centre (CCDC) 623889, 661017, 661018, and 661019 contain the supplementary crystallographic data for this paper. These data can be obtained free of charge via www.ccdc.cam.ac.uk/data_request/cif, by e-mailing, or by contacting The Cambridge Crystallographic Data Centre, 12, Union Road, Cambridge CB2 1EZ, U.K.; fax, +44-1223-336033.

Supporting Information Available: Table of crystallographic data collection and refinement, packing diagrams of crystal structures of compounds, and further mass spectral data. This material is available free of charge via the Internet at http://pubs.acs.org.

JA711254Q

(58) Bancroft, D. P.; Lepre, C. A.; Lippard, S. *J. Am. Chem. Soc.* **1990**, *112*, 6860–6871.
(59) Eastman, A. *Chem.-Biol. Interact.* **1987**, *61*, 241–248.
(60) Vahrenkamp, H. *Dalton Trans.* **2007**, *42*, 4751–4759.